

## A Robust Roll Stabilization Controller with Aerodynamic Disturbance and Actuator Failure Consideration

Qiancai Ma<sup>1</sup>, Fengjie Gao<sup>2</sup>, Yang Wang<sup>3</sup>, Qiuxiong Gou<sup>3</sup> and Liangyu Zhao<sup>1,\*</sup>

**Abstract:** Combining adaptive theory with an advanced second-order sliding mode control algorithm, a roll stabilization controller with aerodynamic disturbance and actuator failure consideration for spinning flight vehicles is proposed in this paper. The presented controller is summarized as an “observer-controller” system. More specifically, an adaptive second-order sliding mode observer is presented to select the proper design parameters and estimate the knowledge of aerodynamic disturbance and actuator failure, while the proposed roll stabilization control scheme can drive both roll angle and rotation rate smoothly converge to the desired value. Theoretical analysis and numerical simulation results demonstrate the effectiveness of the proposed controller.

**Keywords:** Roll stabilization, fault-tolerant control, aerodynamic disturbance, actuator failure, precision strike.

### 1 Introduction

In modern warfare, the precision strike is still a challenge for guided spinning flight vehicles. The nonlinearities and uncertainties of the aerodynamic disturbance in Clare et al. [Clare, Ingram and Nicolaides (1970)] caused by the high angle of attack maneuver may affect the roll stabilization, reduce the impact accuracy and the shooting range, even lead to a catastrophic flight. To enhance flight performance, it is still a challenge to realize roll stabilization.

Based on linear control theory, traditional roll stabilization controllers in Nesline et al. [Nesline and Zarchan (1984); Mracek and Ridgely (2005)] are designed by ignoring the aerodynamic disturbance. These controllers can guarantee stability and performance at a small angle of attack, but the performances of these controllers are quite difficult to be ensured since the aerodynamic coefficient changes rapidly at a high angle of attack, according to the work in Ericsson [Ericsson (1985)].

Because of the inherent strong robustness against external disturbances and uncertainties, sliding mode control (SMC) in Levant et al. [Levant (2001); Shima, Idan and Golan (2006)] is a powerful tool for roll stabilization control. Then second-order sliding mode control (STA) in Shtessel et al. [Shtessel, Shkolnikov and Levant (2009); Trivedi,

---

<sup>1</sup> School of Aerospace Engineering, Beijing Institute of Technology, Beijing, 100081, China.

<sup>2</sup> Hiwing Aviation General Equipment Co. Ltd., Beijing, 100074, China.

<sup>3</sup> Xi'an Modern Control Technology Research Institute, Xi'an, 710054, China.

\* Corresponding Author: Liangyu Zhao. Email: zhaoly@bit.edu.cn.

Received: 29 July 2019; Accepted: 15 November 2019.

Bandyopadhyay, Chaudhuri et al. (2015)] is adopted to design autopilot to guarantee roll stabilization. STA generates the continuous control function that drives the sliding variable and its derivative to zero in finite time in the presence of the smoothly matched disturbances with bounded gradient, but the boundary of the gradient should be known in advance. However, due to physical limitations, aerodynamic parameters are difficult to measure in real-time.

All of the above methods and theories pay attention to the aerodynamic disturbance, and the real manipulation disturbances should also be taken into account. As a kind of common manipulation disturbance, actuator failures may cause severe performance deterioration of control systems, and even lead to catastrophic accidents. To accommodate actuator failures, fault diagnosis-based approaches in Wu et al. [Wu, Zhang and Zhou (2000); Cao, Guo and Wen (2011)], learning-based approaches in Polycarpou [Polycarpou (2001)] and sliding mode control-based approaches in Corradini et al. [Corradini and Orlando (2007)] have been proposed. For actuator stuck faults, an adaptive fault-tolerant control scheme by introducing an iterative learning observer has also been proposed in Chen et al. [Chen and Jiang (2005)]. However, to design the above approaches, the knowledge of lower and upper bounds of the actuator efficiency factor is needed as well.

Inspired by the above work, a robust roll stabilization controller is proposed with aerodynamic disturbance and actuator failure consideration is proposed in this paper. The main contributions of this paper can be concluded as follows: (1) an “observer-controller” system in which an adaptive second-order sliding mode observer is presented to select the proper design parameter and estimate the knowledge of aerodynamic disturbance and actuator failure; (2) the proposed roll stabilization control scheme drives both roll angle and rotation rate smoothly to converge to the desired value.

The rest of this paper is organized as follows. In Section 2, the kinematics model of spinning flight vehicle and actuator failure during the flight phase are introduced. In Section 3, an adaptive second-order sliding mode observer and a robust roll stabilization controller are declared. Simulation results are provided and analyzed in Section 4. Some conclusions are made in the last section.

## **2 Problem formulation**

In this section, the kinematics model of spinning flight vehicle and actuator failure during the flight phase are presented for the roll stabilization controller design. Moreover, some assumptions and lemmas are also considered for further application to facilitate the design.

### ***2.1 Kinematics model of spinning flight vehicle***

According to Trivedi et al. [Trivedi, Bandyopadhyay, Chaudhuri et al. (2015)], the kinematics model of spinning flight vehicle considering aerodynamic disturbance at a high angle of attack can be described as follow:

$$\ddot{\phi} = -\omega_{RR}\dot{\phi} + K_{\delta}\delta + Cl_a \sin(4\phi) \quad (1)$$

where  $\phi$  and  $\delta$  denote the roll angle and actuator deflection angle,  $\omega_{RR}$ ,  $K_\delta$  and  $Cl_a$  represent actuator bandwidth, fin effectiveness and aerodynamic coefficient. The last term,  $Cl_a \sin(4\phi)$ , is an aerodynamic disturbance, which is usually ignored by assuming a small  $\phi$ . Since the coefficient increases rapidly at a high angle of attack, small variations in  $\phi$  can cause large disturbances [Kang, Kim, Won et al. (2008)].

In this study, it is assumed that the signals,  $\phi$ ,  $\dot{\phi}$  and  $\delta$  can be measured. Let  $\phi_d$  and  $\dot{\phi}_d$  denote the desired roll angle and rotation rate,  $x_1$  and  $x_2$  represent the roll angle error and rate error, which are defined by  $x_1 = \phi - \phi_d$  and  $x_2 = \dot{\phi} - \dot{\phi}_d$ , respectively, then the system (1) can be rewritten as

$$\begin{aligned} \dot{x}_1 &= x_2 \\ \dot{x}_2 &= -\omega_{RR}x_2 + K_\delta\delta + \Delta \end{aligned} \quad (2)$$

where  $\Delta$  denotes the disturbance term, and  $\Delta = Cl_a \sin(4x_1)$ .

Owing to the physical limits, the disturbance term  $\Delta$  is bounded. The objective of this study can be described as designing actuator deflection angles command  $\delta$  for the system (2) aiming to drive the roll angle and its rate to the desired value.

## **2.2 Actuator faults**

Owing to the inherent properties, time delay, sensor failure and other reasons, actuator failure, occurs frequently and may result in undesirable performance during the control phase. According to the engineering experience, actuator failure usually shows up as four forms: saturation, nonlinearity, discontinuous and indeterminacy. Based on control theory and control system, and taking actuator faults into account, the total actuator deflection can be formulated as the following form [Li and Yang (2012)]:

$$\delta(t) = \rho\delta(t) + \sigma\delta_s(t) \quad (3)$$

where  $\rho$  denotes the unknown bounded time-varying actuator efficiency and  $\sigma\delta_s$  represents the bounded time-varying stuck fault. To cope with the system (2) in the presence of the actuator failure as Eq. (3), a new actuator failure consideration system is defined as:

$$\begin{aligned} \dot{x}_1 &= x_2 \\ \dot{x}_2 &= -\omega_{RR}x_2 + K_\delta\rho\delta(t) + K_\delta\sigma\delta_s(t) + \Delta \end{aligned} \quad (4)$$

This completes the control system in the presence of actuator failure during the roll stabilization phase.

Owing to the physical limits, one can see that the dumped disturbance  $\Delta$  and its first-order time derivative is continuous and bounded but unknown, i.e., there exist two positive constant  $\Delta_{\max}$  and  $\dot{\Delta}_{\max}$  satisfied  $\Delta < \Delta_{\max}$  and  $\dot{\Delta} < \dot{\Delta}_{\max}$ , respectively.

### 2.3 Preliminaries

**Notation 1.** Throughout this paper, following notation will be used. For any given vector  $\mathbf{x} = [x_1, x_2, \dots, x_n]^T$ , its absolute value is denoted as  $|\mathbf{x}| = [|x_1|, |x_2|, \dots, |x_n|]^T$ , its vectorial time derivative is denoted as  $\dot{\mathbf{x}} = [\dot{x}_1, \dot{x}_2, \dots, \dot{x}_n]^T$ , its reciprocal value is denoted as  $\mathbf{x}^{-1} = [x_1^{-1}, x_2^{-1}, \dots, x_n^{-1}]^T$ , its 2-norm is denoted as  $\|\mathbf{x}\| = \sqrt{\mathbf{x}^T \mathbf{x}}$ , its vectorial sign function is denoted as  $\text{sgn}(\mathbf{x}) = [\text{sgn}(x_1), \text{sgn}(x_2), \dots, \text{sgn}(x_n)]^T$ , its maximum values are denoted as  $\lambda_{\max}(\mathbf{x}) = \text{col}(\lambda_{\max}(x_1), \lambda_{\max}(x_2), \dots, \lambda_{\max}(x_n))$ , and its minimum values are denoted as  $\lambda_{\min}(\mathbf{x}) = \text{col}(\lambda_{\min}(x_1), \lambda_{\min}(x_2), \dots, \lambda_{\min}(x_n))$ .

**Notation 2.** For two any given column vector  $\mathbf{A} = [a_1, a_2, \dots, a_n]^T$  and  $\mathbf{B} = [b_1, b_2, \dots, b_n]^T$  with the same length, in this paper,  $\mathbf{A} \geq \mathbf{B}$  ( $\mathbf{A} \leq \mathbf{B}$ ) is defined as that every element in  $\mathbf{A}$  is larger (smaller) than or equal to the element in  $\mathbf{B}$  with the corresponding position, i.e.,  $a_1 \geq b_1, a_2 \geq b_2, \dots, a_n \geq b_n$  ( $a_1 \leq b_1, a_2 \leq b_2, \dots, a_n \leq b_n$ ). For an arbitrary column vector  $\mathbf{A} = [a_1, a_2, \dots, a_n]^T$  and any given constant  $m$ ,  $\mathbf{A} \geq m$  ( $\mathbf{A} \leq m$ ) means that every element in  $\mathbf{A}$  is larger (smaller) than or equal to  $m$ .

**Lemma 1** [Li and Tian (2007)]. Considering the nonlinear system  $\dot{x} = f(x, t)$ ,  $x \in R^n$ . Assume the existence of a continuous and positive definite function  $V(x)$ ,

$$\dot{V}(x) + \lambda_1 V(x) + \lambda_2 V^\theta(x) \leq 0 \quad (5)$$

where  $\lambda_1, \lambda_2 > 0$  and  $0 < \theta < 1$  are constants.  $x(t_0) = x_0$ , in which  $t_0$  is the initial time. Then, the time of the system states arriving at the equilibrium point  $T$  satisfies the following inequality:

$$T \leq \frac{1}{\lambda_1(1-\theta)} \ln \left( 1 + \frac{\lambda_1}{\lambda_2} V^{1-\theta}(x_0) \right) \quad (6)$$

**Lemma 2** (Rayleigh's inequality). For any function  $f(\mathbf{x}) = \mathbf{x}^T \mathbf{P} \mathbf{x}$  where n-dimension nonsingular matrix  $\mathbf{P}$  is positive-defined, following inequality holds

$$\lambda_{\min}(\mathbf{P}) \|\mathbf{x}\|^2 \leq f(\mathbf{x}) \leq \lambda_{\max}(\mathbf{P}) \|\mathbf{x}\|^2 \quad (7)$$

**Lemma 3** (LaSalle's invariance principle). For arbitrary given autonomous system and scalar function  $V(x)$ , denote two sets as  $\Omega_l = \{x | V(x) \leq l\}$  and  $S = \{x | \dot{V}(x) = 0, x \in \Omega_l\} \subset \Omega_l$  in system state space, respectively. If there is a continuous differentiable scalar function  $W(x)$  such that:

(1). There is a properly chosen positive constant  $l_0$  such that  $\Omega_{l_0}$  is bounded,

(2).  $W(x) \leq 0, \forall x \in \Omega_{i_0}$ .

Then for the arbitrary initial state  $x(0) \in \Omega_{i_0}$ , the system trajectory  $x(t)$  will approach the maximum invariable set  $M$  in the presence of  $t \rightarrow \infty$ , where  $M$  is the union of all of the invariable sets in  $S$ .

### 3 Robust finite time convergent roll stabilization controller

In this section, an adaptive second-order sliding mode observer is proposed to estimate the information of the aerodynamic disturbance and actuator failure while a robust roll stabilization controller is presented to drive the roll angle and its rate to the desired value.

#### 3.1 Adaptive second-order sliding mode observer

Considering roll stabilization control system (4), motivated by the works in He et al. [He and Lin (2016)] and Wang et al. [Wang, Ji, Shi et al. (2017)], a second-order sliding mode observer is proposed as follow:

$$\begin{aligned} \dot{\hat{x}}_2 &= \hat{\Delta} + a_1 |x_2 - \hat{x}_2|^{1-1/k} \text{sign}(x_2 - \hat{x}_2) - \omega_{RR} x_2 + K_\delta \delta \\ \dot{\hat{\Delta}} &= a_2 |x_2 - \hat{x}_2|^{1-2/k} \text{sign}(x_2 - \hat{x}_2) \end{aligned} \quad (8)$$

where  $\hat{x}_2$  and  $\hat{\Delta}$  are the estimations of the  $x_2$  and  $\Delta$ ,  $a_1$ ,  $a_2$  and  $k$  are positive constants.

According to the conclusion of He et al. [He and Lin (2016)], the proposed observer can estimate the disturbance  $\Delta$  with high precision. However, how to choose  $a_1$  and  $a_2$  is still a tough question to cope with. To overcome this problem, we proposed observer (8) and came up with an adaptive observer which can adjust the design parameters itself and is formulated as:

$$\begin{aligned} \dot{\hat{x}}_2 &= \hat{\Delta} + a_1(t) |x_2 - \hat{x}_2|^{1-1/k} \text{sign}(x_2 - \hat{x}_2) - \omega_{RR} x_2 + K_\delta \delta \\ \dot{\hat{\Delta}} &= a_2(t) |x_2 - \hat{x}_2|^{1-2/k} \text{sign}(x_2 - \hat{x}_2) \end{aligned} \quad (9)$$

where  $a_1(t) = c_1 \sqrt{L(t)}$  and  $a_2(t) = c_2 L(t)$ . And the adaptive gain is proposed as:

$$L(t) = l \cdot \text{sgn}(\|\mathbf{x}\| - \varepsilon) \quad (10)$$

where  $m > 0$  is used to regulate the adaptive process,  $L(t) > 0$  is defined as an adaptive parameter,  $\varepsilon$  is a small value to ensure that  $L(t)$  will be bound.

**Proposition 1.** Considering the adaptive law Eq. (10), the adaptive parameter  $L(t)$  is globally bounded.

**Proof.** At the initial phase of control,  $L(t)$  will rise gradually and drive the rotation rate to converge, when the adaptive law works. When the system state satisfies  $\|\mathbf{x}\| \leq \varepsilon$ , the term  $\text{sgn}(\|\mathbf{x}\| - \varepsilon)$  turns into negative and the adaptive parameter  $L(t)$  pushes  $\mathbf{x}$  to

converge into the region  $\|x\| < \varepsilon$ . On the other hand, if  $L(t)$  is too small to resist the external disturbance, the adaptive law Eq. (10) will raise  $L(t)$  until the force the system state converge to the region  $\|x\| < \varepsilon$ . Thus the adaptive parameter  $L(t)$  is always bound and cannot increase to infinity.

The property of the proposed adaptive law is summarized as the following theorem.

**Theorem 1.** Denote  $e_1 = x_2 - \hat{x}_2$  and  $e_2 = \Delta - \hat{\Delta}$  represent the estimation errors, and  $e = [e_1, e_2]^T$ . The estimation errors will approach the following region in finite time in the presence of **Proposition 1**.

$$\|e\| \leq \left( \frac{\Delta_{\max} \|B\|}{\lambda_{\min}(M)} \right)^{(k-1)/(k-2)} \quad (11)$$

where

$$M = \begin{bmatrix} c_1 c_2 L^{3/2} + c_1^3 L^{3/2} \frac{k-1}{k} & -c_1^2 L^{3/2} \frac{k-1}{k} \\ -c_1^2 L^{3/2} \frac{k-1}{k} & c_1 L^{1/2} \frac{k-1}{k} \end{bmatrix}, B = \begin{bmatrix} -c_1 L^{1/2} \\ 2 \end{bmatrix}$$

**Proof.** See Appendix A.

**Remark 1.** For the stage where it follows from  $e_1 = 0$  and  $\hat{\Delta} = 0$ , according to Eq. (11) and (A.6) that  $e_1 = e_2 = 0$ , which represents the proposed observer will not work or affect the control system.

### 3.2 Roll stabilization controller design

Define a sliding manifold as:

$$s = x_2 + d_1 x_1 + d_2 |x_1|^{d_3} \text{sign}(x_1) \quad (12)$$

The time derivative of  $s$  can be expressed as:

$$\begin{aligned} \dot{s} &= \dot{x}_2 + d_1 \dot{x}_1 + d_2 d_3 |x_1|^{d_3-1} x_2 \\ &= F(x_1, x_2) + K_\delta \delta \end{aligned} \quad (13)$$

where

$$F(x_1, x_2) = -\omega_{RR} x_2 + d_1 x_2 + d_2 d_3 |x_1|^{d_3-1} x_2 + \Delta \quad (14)$$

For the reconstructed control system, a novel robust roll stabilization control scheme can be formulated by,

$$\begin{aligned}\delta &= -\frac{1}{K_\delta}(F(x_1, x_2) - u) \\ u(t) &= -b_1 s^{1-1/\tau} \operatorname{sgn}(s) + \xi \\ \dot{\xi} &= -b_2 |s|^{1-2/\tau} \operatorname{sgn}(s)\end{aligned}\tag{15}$$

where  $d_1, d_2, d_3, b_1, b_2$  and  $\tau$  are positive constants.

### 3.3 Design of roll stabilization controller

The main conclusion of this part is summarized as the following theorem.

**Theorem 2.** Considering the control system (4), the adaptive second-order sliding mode observer (9) and the roll stabilization control scheme (15) with the sliding manifold (12), then the sliding surface will converge to a small region around zero in finite time.

**Proof.** Considering the ‘‘observer-controller’’ system, the proof of the **Theorem 2.** should be divided into two steps. First, the boundedness of the states of the closed-loop system in any time region  $[0, t]$  is verified via the finite-time bounded function in **Lemma 1**; second, the finite-time convergent property is verified via the strict Lyapunov function.

*Step 1.* Substituting (15) into (13) yield

$$\dot{s} = \dot{\Delta} - \dot{\hat{\Delta}} - b_1 |s|^{1-1/\tau} \operatorname{sgn}(s) - b_2 \int |s|^{1-2/\tau} \operatorname{sgn}(s) dt\tag{16}$$

For ease of following proof, introduce two auxiliary vectors  $\mathbf{y} = [y_1, y_2]^T \in \mathbb{R}^2$  as

$$\begin{aligned}y_1 &= s \\ y_2 &= \dot{\Delta} - \dot{\hat{\Delta}} - b_2 \int |s|^{1-2/\tau} \operatorname{sgn}(s) dt\end{aligned}\tag{17}$$

Then take the derivative of (17) with respect to time, yield

$$\begin{aligned}\dot{y}_1 &= y_2 - b_1 |s|^{1-1/\tau} \operatorname{sgn}(s) \\ \dot{y}_2 &= \dot{\Delta} - \dot{\hat{\Delta}} - b_2 |s|^{1-2/\tau} \operatorname{sgn}(s)\end{aligned}\tag{18}$$

Denote  $\mathbf{y} = \left[ |y_1|^{1-1/\tau} \operatorname{sgn}(y_1) \quad y_2 \right]^T$ , then take the following finite-time bounded function into account.

$$V_1 = |y_1|^{2(\tau-1)/\tau} + y_2^2\tag{19}$$

Take the time derivative of  $V_1$ , yields

$$\begin{aligned}\dot{V}_1 &= 2 \frac{\tau-1}{\tau} |y_1|^{1-2/\tau} \operatorname{sgn}(y_1) \cdot (y_2 - b_1 |y_1|^{1-1/\tau} \operatorname{sgn}(y_1)) + 2y_2 (\dot{\Delta} - \dot{\hat{\Delta}} - b_2 |y_1|^{1-2/\tau} \operatorname{sgn}(y_1)) \\ &\leq 2 \frac{\tau-1}{\tau} |y_1|^{1-2/\tau} \operatorname{sgn}(y_1) \cdot y_2 + 2y_2 (\dot{\Delta} - \dot{\hat{\Delta}} - b_2 |y_1|^{1-2/\tau} \operatorname{sgn}(y_1)) \\ &\leq 2 \frac{\tau-1}{\tau} |y_1|^{1-2/\tau} \operatorname{sgn}(y_1) \cdot y_2 + 2|y_2| |\dot{\Delta} - \dot{\hat{\Delta}}| + 2b_2 |y_1|^{1-2/\tau} \operatorname{sgn}(y_1) \cdot |y_2|\end{aligned}\tag{20}$$

According to **Lemma 3** and the inequality  $a^2 + b^2 \geq 2ab$

$$\begin{aligned} \dot{V}_1 \leq & 2 \frac{\tau-1}{\tau} \left( \frac{\tau-2}{2(\tau-1)} |y_1|^{2(\tau-1)/\tau} + \frac{\tau}{2(\tau-1)} |y_2|^{2(\tau-1)/\tau} \right) + |y_2|^2 + \left| \dot{\Delta} - \hat{\Delta} \right|^2 \\ & + 2 \frac{b_2}{\tau} \left( \frac{\tau-2}{2(\tau-1)} |y_1|^{2(\tau-1)/\tau} + \frac{\tau}{2(\tau-1)} |y_2|^{2(\tau-1)/\tau} \right) \end{aligned} \quad (21)$$

Next, take the following two cases into account.

Case 1.  $|y_2| \geq 1$ . According to  $2(\tau-1)/\tau \in (1,2)$ , one can imply that  $|y_2|^{2(\tau-1)/\tau} \leq |y_2|^2$ . Substituting this inequality into (21) yield

$$\begin{aligned} \dot{V}_1 \leq & \left( \frac{\tau-2}{\tau} + \frac{(\tau-2)b_2}{\tau-1} \right) |y_1|^{2(\tau-1)/\tau} + \left( 2 + \frac{b_2\tau}{\tau-1} \right) |y_1|^2 + \left| \dot{\Delta}_1 - \hat{\Delta}_1 \right|^2 \\ \leq & K_1 V_1 + \left| \dot{\Delta}_1 - \hat{\Delta}_1 \right|^2 \end{aligned} \quad (22)$$

$$\text{with } K_1 = \max \left\{ \frac{\tau-2}{\tau} + \frac{(\tau-2)b_2}{\tau-1}, 2 + \frac{b_2\tau}{\tau-1} \right\}$$

Case 2.  $|y_2| < 1$ . According to  $2(\tau-1)/\tau \in (1,2)$  one can imply that  $|y_2|^{2(\tau-1)/\tau} \leq 1$ . Substitute this inequality into (21) yield

$$\begin{aligned} \dot{V}_1 \leq & \left( \frac{\tau-2}{\tau} + \frac{(\tau-2)b_2}{\tau-1} \right) |y_1|^{2(\tau-1)/\tau} + \left( 1 + \frac{b_2\tau}{\tau-1} \right) + |y_1|^2 + \left| \dot{\Delta}_1 - \hat{\Delta}_1 \right|^2 \\ \leq & K_2 V_1 + \left( 1 + \frac{b_2\tau}{\tau-1} \right) + \left| \dot{\Delta}_1 - \hat{\Delta}_1 \right|^2 \end{aligned} \quad (23)$$

$$\text{with } K_2 = \max \left\{ \frac{\tau-2}{\tau} + \frac{(\tau-2)b_2}{\tau-1}, 1 \right\}.$$

It follows for **Proposition 1** that  $\left| \dot{\Delta}_1 - \hat{\Delta}_1 \right|$  is continuous, differentiable and unlimited ultimate bounded, thus,  $\left| \dot{\Delta}_1 - \hat{\Delta}_1 \right|$  is unlimited ultimate bounded. Assume there exists a large enough positive constant  $\left| \dot{\Delta}_1 - \hat{\Delta}_1 \right| \leq \hat{\Delta}_{\max}$ . Combining Case 1 and Case 2 yields,

$$\dot{V}_1 \leq K_1 V_1 + L_1 \quad (24)$$

$$\text{with } K = \max \{K_1, K_2\} \text{ and } L_1 = \left( 1 + \frac{b_2\tau}{\tau-1} \right) + \hat{\Delta}_{\max}^2.$$

Solving the inequality (24) in arbitrary time region  $[0, t]$  yields,

$$V_1 \leq \left( V_1(0) + \frac{L_1}{K_1} \right) e^{K_1 t} - \frac{L_1}{K_1} \quad (25)$$

where  $V_1(0)$  is the initial value of  $V_1$ . From the Eq. (25), one can conclude that the ‘‘observer-controller’’ system is bounded.

*Step 2.* It follows for **Proposition 1** that  $\hat{\Delta}$  will converge to a small region around  $\Delta$  in finite time and the term  $|\dot{\hat{\Delta}}_1 - \dot{\Delta}_1|$  can be omitted when the system is stable. Combining with the conclusion of Step 1, the system (9) can be degraded as

$$\begin{aligned} \dot{y}_1 &= y_2 - b_1 |s|^{1-1/\tau} \operatorname{sgn}(s) \\ \dot{y}_2 &= -b_2 |s|^{1-2/\tau} \operatorname{sgn}(s) \end{aligned} \quad (26)$$

Consider the following Lyapunov function

$$V_2 = \frac{b_2 \tau}{\tau - 1} |y_1|^{2(1-\tau)/\tau} + \frac{1}{2} |y_2|^2 + \frac{1}{2} \left( b_1 |y_1|^{(1-\tau)/\tau} \operatorname{sgn}(y_1) - y_2 \right)^2 \quad (27)$$

Similarly to  $V_1$ ,  $V_2$  is a semi-positive and continuous, so that  $V_2$  can be used to evaluate the stability of the system.

Taking the derivative of  $V_2$  with respect to time yields,

$$\begin{aligned} \dot{V}_2 &= \left( \frac{b_2 \tau}{\tau - 1} + \frac{1}{2} b_1^2 \right) \frac{2(\tau - 2)}{\tau} |y_1|^{(\tau-1)/\tau} \operatorname{sgn}(y_1) \dot{y}_1 + 2y_2 \dot{y}_2 \\ &\quad - b_1 |y_1|^{(\tau-1)/\tau} \operatorname{sgn}(y_1) \dot{y}_2 - b_1 \frac{\tau - 1}{\tau} |y_1|^{-1/\tau} y_2 \dot{y}_1 \\ &= -|y_1|^{-1/\tau} \left( b_1 b_2 |y_1|^{2(\tau-1)/\tau} + \frac{\tau - 1}{\tau} b_1^3 |y_1|^{2(\tau-1)/\tau} - 2 \frac{\tau - 2}{\tau} b_1^2 |y_1|^{(\tau-1)/\tau} \operatorname{sgn}(y_1) y_2 + \frac{\tau - 1}{\tau} b_1 |y_2|^2 \right) \end{aligned} \quad (28)$$

Rewrite (28) into matrix form as

$$\dot{V}_2 = -|y_1|^{-1/\tau} \mathbf{v}^T \mathbf{P} \mathbf{v} \quad (29)$$

where  $\mathbf{v} = [y_1, y_2]^T \in \mathbb{R}^2$  and

$$\mathbf{P} = \begin{bmatrix} b_1 b_2 + b_1^3 \frac{\tau - 1}{\tau} & -b_1^2 \frac{\tau - 1}{\tau} \\ -b_1^2 \frac{\tau - 1}{\tau} & b_1 \frac{\tau - 1}{\tau} \end{bmatrix}$$

It follows from  $b_1 > 0$ ,  $b_2 > 0$  and  $\tau > 0$  that  $P$  is positive define.

Rewrite  $V_2$  as following matrix form,

$$V_2 = \mathbf{v}^T \mathbf{Q} \mathbf{v} \quad (30)$$

where

$$Q = \frac{1}{2} \begin{bmatrix} \frac{b_2 \tau}{\tau - 1} + b_1^2 & -b_1 \\ -b_1 & 2 \end{bmatrix}$$

It follows from  $b_1 > 0$ ,  $b_2 > 0$  and  $\tau > 0$  that  $Q$  is positive definite and  $V_2$  is radially unbounded, so that

$$\lambda_{\min}(Q) \|\mathbf{v}\|^2 \leq V_2 \leq \lambda_{\max}(Q) \|\mathbf{v}\|^2 \quad (31)$$

According to  $\|\mathbf{v}\| = \sqrt{|y_1|^{2(\tau-1)/\tau} + y_2^2} \geq |y_1|^{(\tau-1)/\tau}$ , one can imply that  $|y_1|^{1/\tau} \geq \|\mathbf{v}\|^{-1/(\tau-1)}$ . Combining Eq. (29) and Eq. (31), one can conclude that

$$\begin{aligned} \dot{V}_2 &\leq -\|\mathbf{v}\|^{-1/(\tau-1)} \lambda_{\min}(\mathbf{P}) \|\mathbf{v}\|^2 \\ &\leq -\lambda_{\min}(\mathbf{P}) \|\mathbf{v}\|^{(2\tau-3)/(\tau-1)} \\ &\leq -\frac{\lambda_{\min}(\mathbf{P})}{[\lambda_{\max}(\mathbf{P})]^{(2\tau-3)/(2\tau-2)}} V_2^{(2\tau-3)/(2\tau-2)} \end{aligned} \quad (32)$$

Since  $(2\tau-3)/(2\tau-2) \in (0, 0.5)$ , according to **Lemma 1**, the rotation rate converges to a small region around zero in finite time. This completes the proof.

## 4 Simulation

In this section, the effectiveness of the proposed robust finite time convergent roll stabilization controller is demonstrated through numerical simulations. The simulations are performed in the MATLAB platform by using a fourth-order Runge-Kutta solver with fixed step size 0.001 s. The variations of the coefficient parameter  $Cl_a$  and  $K_\delta$  to flight time are similar to the flight condition in Trivedi et al. [Trivedi, Bandyopadhyay, Chaudhuri et al. (2015)].

### 4.1 Simulation for disturbance coefficient

To verify the effectiveness of the proposed roll stabilization controller to deal with disturbance coefficient, simulations considering different angles of attack are performed. Two kinds of desired rotation rate were taken into account to demonstrate the general applicability and robustness of the proposed controller, which could be expressed as follows,

Case 1:  $\phi(0) = 22.5^\circ$ ,  $\dot{\phi}(0) = 0(\text{rad/s})$ ,  $\phi_a = 0^\circ$ ,  $\dot{\phi}_a = 0(\text{rad/s})$ ;

Case 2:  $\phi(0) = 0^\circ$ ,  $\dot{\phi}(0) = 4\pi(\text{rad/s})$ ,  $\phi_a = 5\pi t(\text{rad})$ ,  $\dot{\phi}_a = 5\pi(\text{rad/s})$ .

The parameters of the proposed roll stabilization controller are given in Tab. 1.

**Table 1:** Roll stabilization controller design parameters

Design parameter	Value	Design parameter	Value
$b_1, b_2$	80,80	$k$	2.1
$c_1, c_2$	1.2,2	$\tau$	2.5
$d_1, d_2, d_3$	4,3,2.3	$l$	0.8 $t$
$\varepsilon$	0.01		

Figs. 1-3 show the simulation result of Case 1. Fig. 1 shows that the roll stabilization controller can drive the roll angle successfully to converge to the desired roll angle. Fig. 2 shows that the roll stabilization controller can drive the rotation rate successfully to converge to the desired one. Fig. 3 shows deflection angles to time. It can be observed that the fin deflection is smooth and converges to a small region around zero within 200 ms.

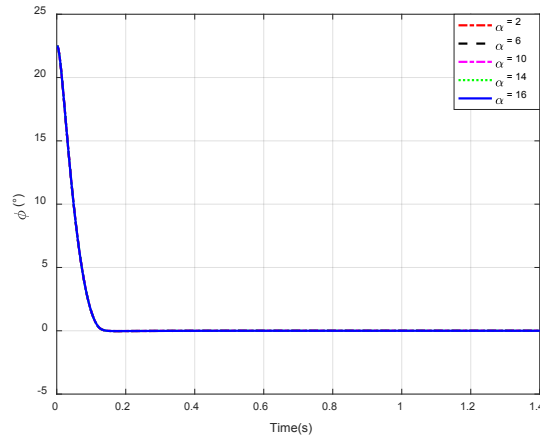


**Figure 1:** Roll angle curves at different angles for Case 1

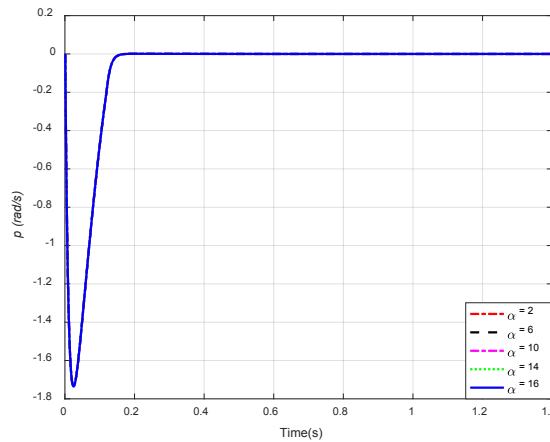


**Figure 2:** Rotation rate curves at different angles for Case 1

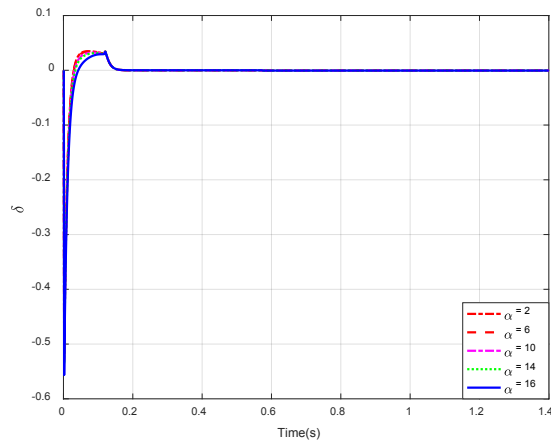


**Figure 3:** Deflection angle curves at different angles for Case 1

Figs. 4-6 show the results of Case 2. Fig. 4 shows that the roll stabilization controller can drive the roll angle successfully to converge to the desired roll angle. Fig. 5 shows that the roll stabilization controller can drive the rotation rate successfully to converge to the desired one. Fig. 6 shows deflection angles to time. It can be observed that the fin deflection is smooth and converges to a small region around zero within 0.15 s. The simulation results of Case 1 and Case 2 show that the roll stabilization controller can get rid of the influence of the disturbance coefficient considering different angles of attack.

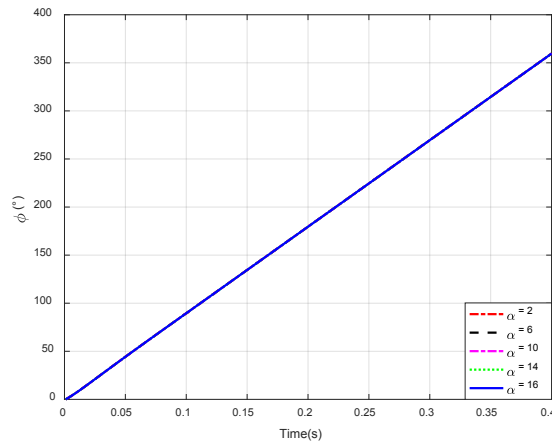


**Figure 4:** Roll angle curves at different angles for Case 2

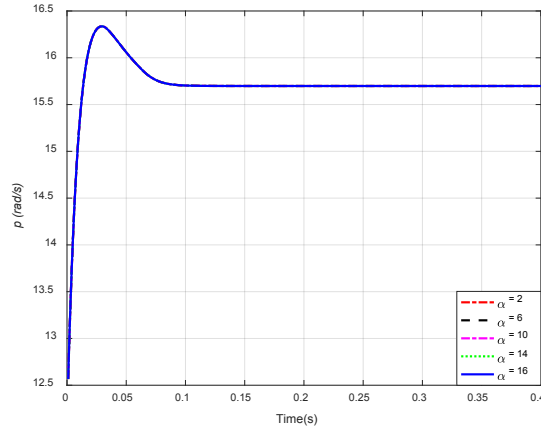


**Figure 5:** Rotation rate curves at different angles for Case 2

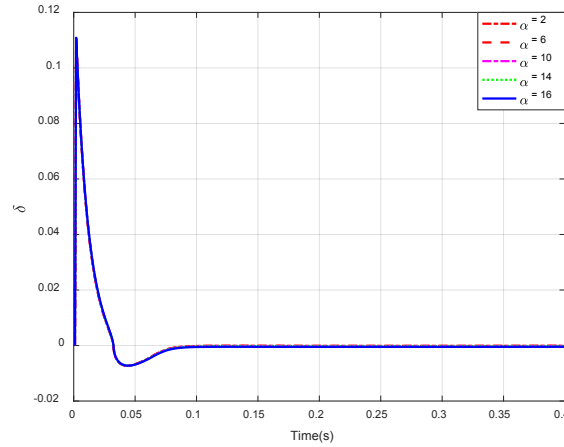


**Figure 6:** Deflection angle curves at different angles for Case 2

#### **4.2 Simulation for loss of actuator efficiency**

The loss of the bounded time-varying actuator efficiency is considered in this simulation, where loses 30% of actuator efficiency, i.e.,  $\rho = 0.7$  and the stuck fault is not considered, i.e.,  $\sigma\delta_s = 0$ .

In order to show the superiority of the proposed roll stabilization controller, a second-order sliding mode observer [He and Lin (2016)] based roll stabilization controller (STWO) is introduced in this simulation as comparisons.

The STWO is defined in the equation below,

$$\begin{aligned} \dot{\hat{x}}_2 &= \hat{\Delta} + f_1 |x_2 - \hat{x}_2|^{1-1/g} \text{sign}(x_2 - \hat{x}_2) - \omega_{RR} x_2 + K_\delta \delta \\ \dot{\hat{\Delta}} &= f_2 |x_2 - \hat{x}_2|^{1-2/g} \text{sign}(x_2 - \hat{x}_2) \end{aligned} \quad (33)$$

where  $f_1 = 40$ ,  $f_2 = 40$  and  $g = 2.1$ .

The parameters of the proposed roll stabilization controller are given in Tab. 1.

The simulation example is set up as follow:

Case 3:  $\phi(0) = 22.5^\circ$ ,  $\dot{\phi}(0) = 0(\text{rad/s})$ ,  $\phi_d = 0(\text{rad})$ ,  $\dot{\phi}_d = 0(\text{rad/s})$ .

The disturbance coefficient are selected where  $\alpha = 16^\circ$

Figs. 7-10 show the simulation results for loss actuator effectiveness. Fig. 7 shows that the proposed roll stabilization controllers can drive the roll angle to converge to the desired roll angle more precisely. Fig. 8 shows that the proposed roll stabilization controllers can drive the rotation rate successfully to converge to the desired value in a shorter time and remain on the desired value. Fig. 9 shows that the proposed roll stabilization controller can drive the deflection angle successfully and smoothly to converge to the desired one within 0.2 s. Fig. 10 shows the profile of the dual-layer adaption gain  $L(t)$ . It can be observed that the adaption gain is bounded and gradually converging. The simulation results of Case 3 show that the roll stabilization controller can drive both roll angle and rate to converge to the desired value smoothly in a short time around 0.2 s considering the loss of actuator efficiency.

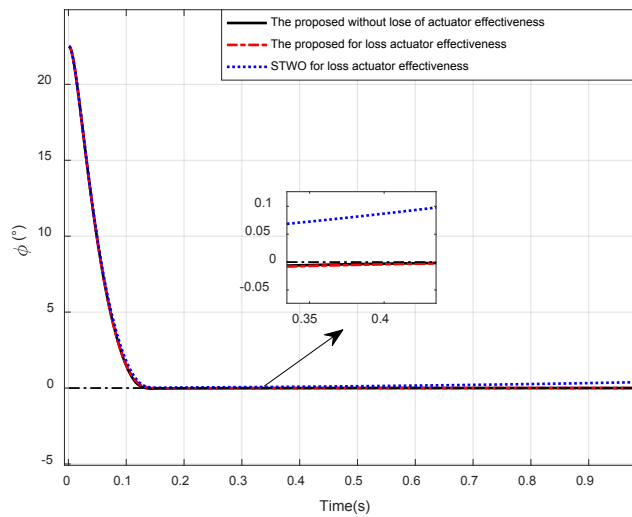


**Figure 7:** Roll angle curves for loss actuator effectiveness

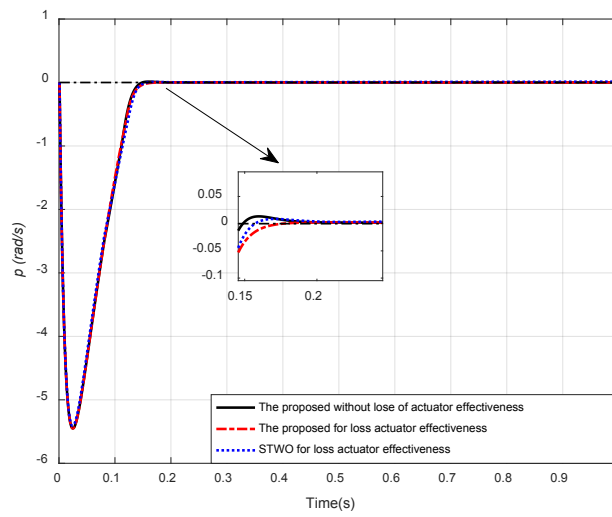


**Figure 8:** Rotation rate curves for loss actuator effectiveness

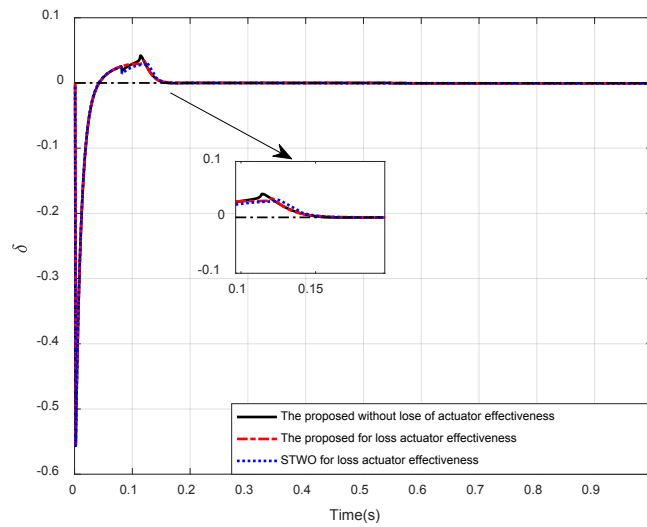


**Figure 9:** Deflection angle curves for loss actuator effectiveness

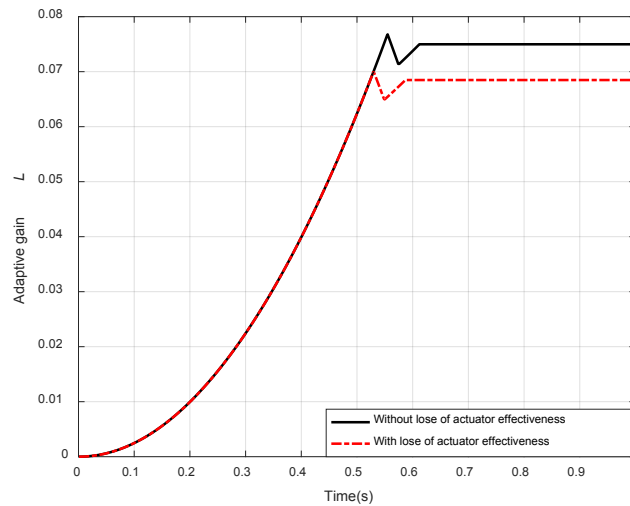


**Figure 10:** The profile of dual-layer adaptive gain

#### 4.3 Simulation for stuck fault

The stuck fault is considered in this simulation, where start at  $t = 0.4s$ , end at  $t = 0.45s$  and deflection angle satisfies  $\delta_s = 0.1\sin(t)$  and the loss of actuator efficiency is not considered.

To show the superiority of the proposed roll stabilization controller, the STWO is proposed in this simulation as comparisons. The parameters of STWO are the same as in Section 4.2.

The parameters of the proposed roll stabilization controller are given in Tab. 1.

The simulation example is set up as in Section 4.2.

The disturbance coefficient is selected where  $\alpha = 16^\circ$

Figs. 11-14 show the simulation results for the stuck fault of the actuator. Fig. 11 shows that the proposed roll stabilization controllers can drive the roll angle to converge to desired roll angle more precisely after the stuck fault. Fig. 12 shows that the proposed roll stabilization controllers can drive the rotation rate successfully to converge to the desired value in a shorter time and remain on the desired value after the stuck fault. Fig. 13 shows that the proposed roll stabilization controller can drive the deflection angle successfully and smoothly to converge to the desired one after the stuck fault. Fig. 14 shows the profile of the dual-layer adaption gain  $L(t)$ . It can be observed that the adaption gain is bounded and gradually converging. The simulation results of Case 3 show that the roll stabilization controller can drive both roll angle and rate to converge to the desired value smoothly in a short time around 0.3 s considering the stuck fault.

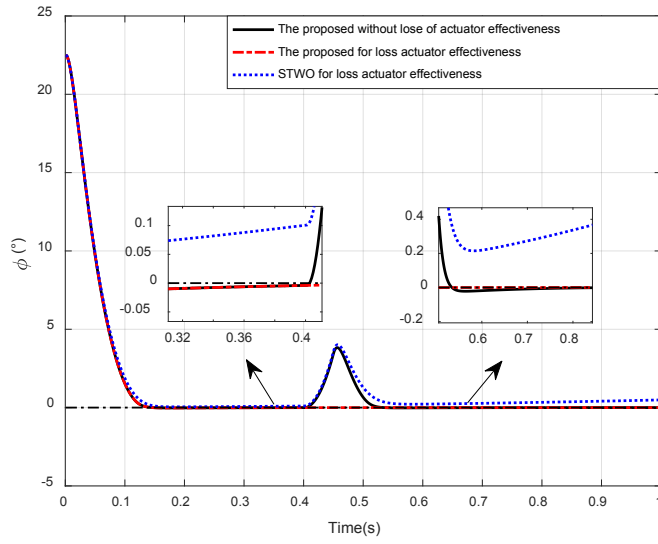


**Figure 11:** Roll angle curves for stuck fault

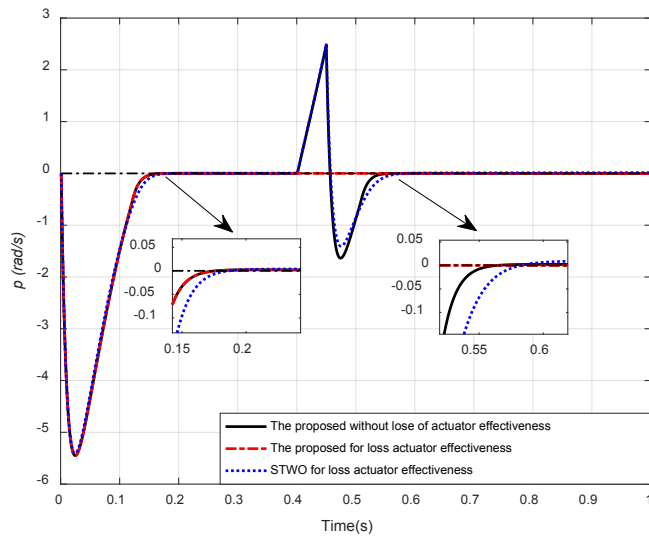


**Figure 12:** Rotation rate curves for stuck fault

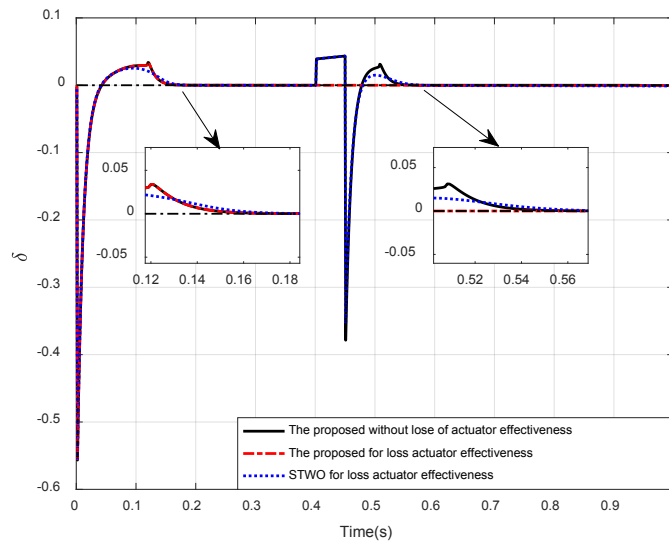


**Figure 13:** Deflection angle curves for stuck fault

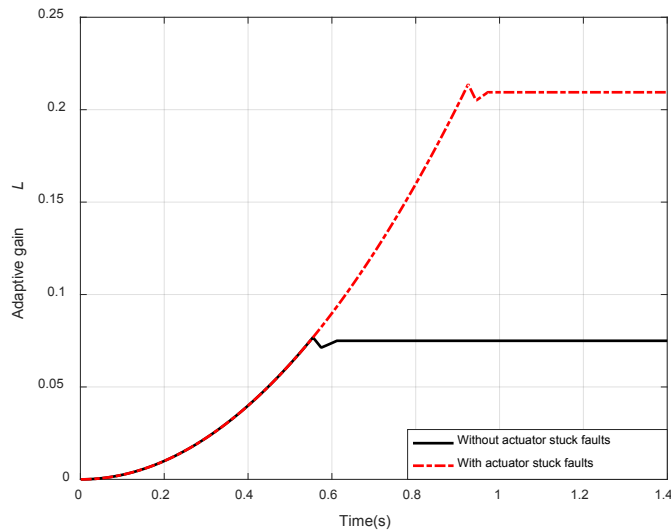


**Figure 14:** The profile of dual-layer adaptive gain

## 5 Conclusions

A robust roll stabilization controller is proposed with disturbance coefficient and actuator failure consideration is proposed in this paper. The details of the proposed roll stabilization controller are summarized as follows: (1) an adaptive second-order sliding mode observer is presented to select the proper design parameter and estimate the knowledge of aerodynamic disturbance and actuator failure; (2) the proposed roll

stabilization control scheme drives both roll angle and rotation rate smoothly to converge to the desired value.

**Acknowledgment:** The grant support from the National Key R&D Program of China (No. 2017YFC0806700), National Natural Science Foundation of China (No. 11532002 and No. 11202023) and Hong Jian Foundation of Xi'an Modern Control Technology Research Institute are greatly acknowledged.

**Conflicts of Interest:** The authors declare that they have no conflicts of interest to report regarding the present study.

## References

- Nicolaidides, J. D.; Ingram, C. W.; Clare, T. A.** (1970): Investigation of the nonlinear flight dynamics of ordnance weapons. *Journal of Spacecraft and Rockets*, vol. 7, no. 10, pp. 1241-1243.
- Nesline, F. W.; Zarchan, P.** (1984): Why modern controllers can go unstable in practice. *Journal of Guidance Control and Dynamics*, vol. 7, no. 4, pp. 495-500.
- Mracek, C. P.; Ridgely, D. B.** (2005): Missile longitudinal autopilots: comparison of multiple three loop topologies. *AIAA Guidance, Navigation, and Control Conference and Exhibit*, pp. 2005-6380.
- Ericsson, L. E.** (1985): Aerodynamic characteristics of noncircular bodies in flat spin and coning motions. *Journal of Aircraft*, vol. 22, no. 5, pp. 387-392.
- Shima, T.; Idan, M.; Golan, O. M.** (2006): Sliding mode control for integrated missile autopilot-guidance. *Journal of Guidance, Control, and Dynamics*, vol. 29, no. 2, pp. 250-260.
- Levant, A.** (2001): Universal SISO sliding-mode controllers with finite-time convergence. *IEEE Transactions on Automatic Control*, vol. 46, no. 9, pp. 1447-1451.
- Shtessel, Y. B.; Shkolnikov, I. A.; Levant, A.** (2009): Guidance and control of missile interceptor using second-order sliding modes. *IEEE Transactions on Aerospace and Electronic Systems*, vol. 45, no. 1, pp. 110-124.
- Trivedi, P. K.; Bandyopadhyay, B.; Chaudhuri, S. K.; Mahata, S. K.** (2015): Roll stabilization: a higher-order sliding-mode approach. *IEEE Transactions on Aerospace and Electronic Systems*, vol. 51, no. 3, pp. 2489-2396.
- Wu, N. E.; Zhang, Y.; Zhou, K.** (2000): Detection, estimation, and accommodation of loss of control effectiveness. *International Journal of Adaptive Control and Signal Processing*, vol. 14, pp. 775-795.
- Cao, S.; Guo, L.; Wen, X.** (2011): Fault tolerant control for disturbance rejection and attenuation performance for systems with multiple disturbances. *Asian Journal of Control*, vol. 13, pp. 1056-1064.
- Polycarpou, M. M.** (2001): Fault accommodation of a class of multivariable nonlinear dynamical systems using a learning approach. *IEEE Transactions on Automatic Control*, vol. 46, no. 5, pp. 736-742.

**Corradini, M. L.; Orlando, G.** (2007): Actuator failure identification and compensation through sliding modes. *IEEE Transactions on Control Systems Technology*, vol. 15, no. 1, pp. 184-190.

**Chen, W.; Jiang, J.** (2005): Fault-tolerant control against stuck actuator faults. *IEE Proceedings-Control Theory and Applications*, vol. 152, pp. 138-146.

**Kang, S.; Kim, H. J.; Won, D.; Tahk, M. J.; Lee, J. et al.** (2008): Robust roll-pitch-yaw integrated autopilot for a high angle-of-attack missile. *AIAA Guidance, Navigation and Control Conference and Exhibit*, vol. 32, no. 5, pp. 1622-1628.

**Li, X.; Yang, G.** (2012): Robust adaptive fault-tolerant control for uncertain linear systems with actuator failures. *IET Control Theory and Applications*, vol. 6, no. 10, pp. 1544-1551.

**Li, S.; Tian, Y.** (2007): Finite-time stability of cascaded time-varying systems. *International Journal of Control*, vol. 80, no. 4, pp. 646-657.

**He, S.; Lin, D.** (2016): Guidance laws based on model predictive control and target manoeuvre estimator. *Transactions of the Institute of Measurement and Control*, vol. 38, no. 12, pp. 1509-1519.

**Wang, W.; Ji, Y.; Shi, Z.; Lin, S.** (2017): A novel approximate finite-time convergent guidance law with actuator fault. *Cluster Computing*, pp. 1-13.

**Appendix A. Proof of Theorem 1**

Take the time derivative of  $e$  yield

$$\dot{e}_1 = e_2 - c_1 \sqrt{L(t)} |e_1|^{1-1/k} \text{sgn}(e_1) \quad (\text{A.1})$$

$$\dot{e}_2 = \dot{\Delta} - c_2 L(t) |e_1|^{1-2/k} \text{sgn}(e_1)$$

Consider following Lyapunov function candidate

$$V_3 = \frac{c_2 L(t) k}{k-1} |e_1|^{2(p-1)/p} + \frac{1}{2} e_2^2 + \frac{1}{2} \left( c_1 \sqrt{L(t)} |e_1|^{(p-1)/p} \text{sgn}(e_1) - e_2 \right)^2 \quad (\text{A.2})$$

Rewrite this equation as the following matrix form

$$V_3 = e^T \Gamma e \quad (\text{A.3})$$

where

$$\Gamma = \frac{1}{2} \begin{bmatrix} \frac{c_2 L(t) k}{k-1} + c_1^2 L(t) & -c_1 \sqrt{L(t)} \\ -c_1 \sqrt{L(t)} & 2 \end{bmatrix}$$

Since  $c_1 > 0, c_2 > 0$  and  $k > 2$ ,  $V_3$  is positive define and radially unbounded.

$$\lambda_{\min}(\Gamma) \|e\|^2 \leq V_3 \leq \lambda_{\max}(\Gamma) \|e\|^2 \quad (\text{A.4})$$

Through similar analysis of  $V_1$  and  $V_2$ , one can imply that  $V_3$  can be used to evaluate the finite-time stability of (10).

Take the derivative of  $V_3$  with respect to time yield

$$\begin{aligned} \dot{V}_3 &= \left( \frac{c_2 L(t) k}{k-1} + \frac{1}{2} c_1^2 L(t) \right) \frac{2(k-1)}{k} |e_1|^{(p-2)/p} \text{sgn}(e_1) \left( e_2 - c_1 \sqrt{L(t)} |e_1|^{(p-1)/p} \text{sgn}(e_1) \right) \\ &\quad + \left( 2e_2 - c_1 \sqrt{L(t)} |e_1|^{(p-1)/p} \text{sgn}(e_1) \right) \times \left( \dot{\Delta} - c_2 L(t) |e_1|^{(p-2)/p} \text{sgn}(e_1) \right) \\ &\quad - c_1 \sqrt{L(t)} \frac{k-1}{k} |e_1|^{-1/p} e_2 \times \left( e_2 - c_1 \sqrt{L(t)} |e_1|^{(p-1)/p} \text{sgn}(e_1) \right) \\ &= -|e_1|^{-1/p} \left( c_1 c_2 L(t)^{3/2} |e_1|^{2(p-1)/p} + \frac{k-1}{k} c_1 L(t)^{3/2} |e_1|^{2(p-1)/p} \right. \\ &\quad \left. - 2 \frac{k-1}{k} c_1^2 L(t) |e_1|^{2(p-1)/p} \text{sgn}(e_1) e_2 + \frac{k-1}{k} c_1 \sqrt{L(t)} e_2^2 \right) \\ &\quad + \left( 2e_2 L(t) - c_1 |e_1|^{2(p-1)/p} \text{sgn}(e_1) \right) \dot{\Delta} \\ &\leq -|e_1|^{-1/p} \left( c_1 c_2 L^{3/2} |e_1|^{2(p-1)/p} + \frac{k-1}{k} c_1 L^{3/2} |e_1|^{2(p-1)/p} \right. \\ &\quad \left. - 2 \frac{k-1}{k} c_1^2 L |e_1|^{2(p-1)/p} \text{sgn}(e_1) e_2 + \frac{k-1}{k} c_1 \sqrt{L(t)} e_2^2 \right) \\ &\quad + \left( 2e_2 L - c_1 |e_1|^{2(p-1)/p} \text{sgn}(e_1) \right) \dot{\Delta}_{\max} \\ &= -|e_1|^{-1/p} e^T M e + \dot{\Delta}_{\max} B e \end{aligned} \quad (\text{A.5})$$

Since  $c_1 > 0, c_2 > 0$  and  $k > 2$ , it is easy to verify that  $\mathbf{M}$  is Hurwitz.

It follows from  $\|e\| = \sqrt{|e_1|^{2(p-1)/p} + e_2^2} \geq |e_1|^{(p-1)/p}$  that  $|e_1|^{1/p} \geq \|e\|^{-1/(p-1)}$ . Combining with (A.4) and (A.5), one can conclude that

$$\begin{aligned} \dot{V}_3 &\leq -\|e\|^{-1/(p-1)} \lambda_{\min}(\mathbf{M}) \|e\|^2 + \dot{\Delta}_{\max} \|\mathbf{B}\| \|e\| \\ &\leq -\left(\lambda_{\min}(\mathbf{M}) \|e\|^{(p-2)/(p-1)} - \dot{\Delta}_{\max} \|\mathbf{B}\|\right) \|e\| \\ &\leq -\left(\lambda_{\min}(\mathbf{M}) \|e\|^{(p-2)/(p-1)} - \dot{\Delta}_{\max} \|\mathbf{B}\|\right) \frac{V_3^{1/2}}{\sqrt{\lambda_{\max}(\Gamma)}} \end{aligned} \quad (\text{A.6})$$

If  $\lambda_{\min}(\mathbf{M}) \|e\|^{(p-2)/(p-1)} - \dot{\Delta}_{\max} \|\mathbf{B}\| > 0$ , (A.6) can be transformed as  $\dot{V}_3 \leq -\frac{\rho V_3^{1/2}}{\sqrt{\lambda_{\max}(\Gamma)}}$ , where

$\rho = \lambda_{\min}(\mathbf{M}) \|e\|^{(p-2)/(p-1)} - \dot{\Delta}_{\max} \|\mathbf{B}\| > 0$ . According to Lemma1, the system rotation rate can

converge into the region  $\|e\| \leq \left(\frac{\dot{\Delta}_{\max} \|\mathbf{B}\|}{\lambda_{\min}(\mathbf{M})}\right)^{(p-2)/(p-1)}$ , this completes the proof.